Lignin Doped Carbon Nanotube Yarns for Improved Thermoelectric Efficiency

*Mario Culebras†, Guang Ren†, Steward O'Connell, Juan J. Vilatela, Maurice N. Collins**

†These authors contributed equally to this work

Dr. M. Culebras, Dr. G. Ren, S. O'Connell, Dr M. N. Collins
Stokes Laboratories, Bernal Institute
University of Limerick
Limerick, V94 T9PX, Ireland
E-mail: maurice.collins@ul.ie

Dr. J. J. Vilatela
IMDEA Materials Institute
Eric Kandel, 2, Tecnogetafe, 28906 Getafe, Madrid, Spain

Keywords: lignin, carbon nanotube, bioelectric

Abstract

Due to ever increasing public awareness of the deteriorating planetary health condition associated with climate change and increasing carbon emissions. Sustainable energy development has come sharply into focus. Here, a thermoelectric material is produced, which consists of macroscopic carbon nanotube yarns (CNTYs) produced continuously from the gas-phase. The CNTYs are doped with lignin, obtained from lignocellulosic waste, and at 23 wt% lignin, electrical conductivity and the Seebeck coefficient are doubled approximately when compared to pristine CNTY samples. As a consequence the power factor has been remarkably improved to 132.2 $\mu W/K^2m$, more than six times that of the pristine CNTY. A thermoelectric generator (TEG) device is manufactured, comprising of twenty CNTY/lignin nanocomposite yarns, and they exhibit a maximum power output of 3.8 μW, at a temperature gradient of 30 K.

1. Introduction

Sustainable energy production and storage is one of the biggest global grand challenges facing society today. Due to ever depleting fossil fuel reserves coupled with climate change associated with increasing CO_2 emissions, there is an urgent requirement for sustainable and efficient energy sources. Currently, 90 % of the world's power is generated by heat engines in which more than two-thirds of the energy produced is lost as heat. Thermoelectric materials offer a solution through harvesting this energy excess and utilising thermal gradients to produce energy due to the Seebeck effect.[1] Whilst, thermoelectric efficiency is measured by the dimensionless figure of merit *ZT*:

$$ZT = \frac{S^2 \sigma T}{\kappa} \quad (1)$$

where *S, T,* σ and κ are the Seebeck coefficient, absolute temperature, electrical conductivity and thermal conductivity respectively. The power factor is calculated as follows:

$$PF = S^2 \sigma \quad (2)$$

and is used to compare the thermoelectric efficiency of samples with similar thermal conductivities. [2] Traditionally, inorganic compounds such as: Bi_2Te_3, PbTe and SiGe have dominated the manufacturing of thermoelectric devices. [3],[4][5],[6] However, serious drawbacks such as: toxicity, scarcity of raw materials and high cost have limited their application and pushed research to newer alternative materials which are highly abundant, low cost and non-toxic. Organic semiconductors such as: conducting polymers, carbonaceous materials and nanocomposites have been proposed as possible candidates due to their availability, low thermal conductivity, ease of chemical modification and scale up potential. Thermoelectric performance of conducting polymers has been increased recently, mainly due to the successful implementation of effective doping mechanisms in PEDOT which enhance electrical conductivity

achieving ZT values of ~ 0.2-0.4.[7] However, these materials are sensitive to humidity and their maximum thermoelectric efficiency is achieved in thin films limiting their practical applications. Carbon based nanostructures, in particular, carbon nanotubes (CNTs) have demonstrated excellent thermoelectric behaviour in multi-layered systems prepared by layer-by-layer (LbL) assembly, in particular materials based on polyaniline (PANI), double-walled carbon nanotubes (DWCNTs) and graphene (1750 $\mu W m^{-1} K^{-2}$), or PANI, DWCNTs, poly(3,4-ethylenedioxythiophene)/poly(styrene sulfonate) (PEDOT:PSS), and graphene (2710 $\mu W m^{-1} K^{-2}$) have shown promise.[8] A particularly attractive architecture are continuous fibres of aligned CNTs, which can achieve tensile properties above synthetic high-performance fibres, mass-normalised electrical conductivity above most metals and high surface areas, amongst other properties. [9] Moreover, as-made yarns of CNTs produced directly from the gas-phase have shown consistently high Seebeck coefficients (50-60 $\mu V\ K^{-1}$), significantly above other nanocarbons and organic materials (38 $\mu V\ K^{-1}$). [8] These yarns are characterised by the extraordinary long length of their CNTs (1mm), which form a continuous porous network of CNT bundled into crystalline stacks. The high degree of perfection of their CNTs results in some low-dimensional behaviour in bulk samples, such as accessible quantum capacitance, sensitivity to adsorbed species and in general strong response to dopants. [10] Indeed, to further increase TE performance CNT yarns have been recently doped with polymers such as: PEDOT:PSS, Poly(ethyleneimine) (PEI), PANI and (poli(3-hexiltiofeno-2,5-diil) P3HT. However, all of these compound are produced from petroleum sources which involves several environmental issues associated to CO_2 emissions, global warming and biodegradability. Therefore, it is difficulty to claim TEGs as sustainable source of energy if the materials used to produced them (or at least part of their components) are not derived from sustainable sources. Looking at this

scenario, this woks propose the use of natural polymers to dope thermoelectric carbon based nanostructures for the first time. In particular, the proposed dopant is lignin, a sustainable biopolymer and a non-valorised by-product of the paper and pulp industry (only 2% of its production is being commercialised in low value products).[11] Lignin is the most abundant aromatic biopolymer on the planet with its structure rendering it ideal for carbon fibre production. [12]

In this work, we found that molecular interactions such as π–π stacking between lignin and CNTY can increase the electrical conductivity and the Seebeck coefficient simultaneously, a fact that is considered the holy grail of thermoelectric materials since both parameters are inversely related. We further elucidate the doping mechanism as a charge carrier filtering effect associated with the incorporation of lignin into the CNT network. This method has the merits of low-cost, sustainability, ease of scale up, and environmental friendliness. The resultant doped CNTYs were investigated in terms of morphology, composition, structure, thermoelectric behavior and power generation. Thus, the present work shows for a first time that lignin is used in the energy harvesting field as a dopant of carbon based semiconductors. This will open up a new paradigm of possibilities for lignin valorization with its use in electronic devices such as thermoelectric generators allowing the production of green energy for a variety of applications including wearable devices and biomedical sensors

2. Results and Discussion

2.1. Morphology

The morphology of pristine CNTY and CNTY/lignin nanocomposites after lignin impregnation were characterised using FE-SEM, as shown in **Figure 1**. The pristine CNTY is composed of long and entangled CNTY bundles with diameters of

approximately 35 nm. However, CNTY/lignin nanocomposites exhibit a smoothed morphology with reduced surface roughness. For impregnated samples (Figure 1b), lignin fills the free volume thereby creating a homogenous film like coating on the CNTs (more FE-SEM images are shown in Figure S1 in the supporting information.). Lignin molecules are known to be highly branched containing structures with a high degree of aromaticity, which allows noncovalent attachment to the CNTY surfaces via strong π-π interactions, as is evidenced in the FTIR results showed in Figure S2 with a clear a shift of the band related to aromatic skeletal vibrations cantered at 1600 cm^{-1} (for pure lignin) to 1594, 1591, 1588, 1588 cm^{-1} for 26, 53, 34 and 23 % of lignin content respectively. These interactions contribute to the efficient formation of highly dense and uniform CNTY/lignin nanocomposites.

2.2. Thermoelectric Properties

To establish the influence of lignin doping of CNTY on its thermoelectric response, the Seebeck coefficient and electrical conductivity of pristine as well as varying lignin dopant contents were measured at room temperature as shown in Figure 1. It can be seen that both the Seebeck coefficient and electrical conductivity of CNTY/lignin nanocomposites vary significantly depending on the lignin dopant concentration. With 13 wt% lignin, the electrical conductivity increases up to 157.6 Scm^{-1}, as revealed in Figure 1d. This is attributed to increased densification and interconnectivity at the nanoscale associated with the strong π-π interactions in the CNTY/lignin nanocomposites, as shown in Figure 1c

It is obvious from the results that doping is a key factor in optimising the thermoelectric behaviour of these materials as it allows tuning of carrier concentration and mobility.

Whilst the lignin itself is not electrically conductive, thereby it is not a negatively impacting on carrier concentration, it contributes to a more efficient pathway for carrier transport through increased CNTY bundle densification and interconnectivity. Furthermore, as shown in Figure 1e, it is likely that when the CNTY interacts with lignin molecules via the aforementioned π–π interactions, the equilibrium energy band at the CNTY/lignin interface is driven towards a lower energy barrier state that ultimately facilitates the mobility of high-energy carriers whilst filtering out low-energy carriers via a carrier filtering effect. [13] Thereby, leading to enhanced charge transport from lignin to CNTY. The electrical conductivity is a result of the balance between reduced carrier concentration and enhanced carrier mobility. At a dopant concentration of 13 wt%, the effect of enhanced carrier mobility surpasses that of reduced carrier concentration, resulting in higher electrical conductivity than that of the pristine CNTY. At higher dopant concentrations, the carrier mobility of nanocomposite is shown to decrease exponentially with increased lignin concentration, this is attributed to the increased tendency of lignin to aggregate, particularly at the surface of the nanocomposite resulting in a deterioration of electrical conductivity. Similar phenomenon have been elsewhere. [14]

All the CNTY /lignin nanocomposites exhibited positive values of Seebeck coefficient, indicating p-type characteristics. Generally, doping is known to affect the Seebeck coefficient by changing the electron density of states (DOS). [3a] Seebeck coefficient (*S*) is expressed as follows:

$$S = \frac{8\pi^2 k_B^2}{3eh^2} m^* T \left(\frac{\pi}{3n}\right)^{\frac{2}{3}} \quad (3)$$

where k_B is the Boltzmann constant, h is the Planck constant, m^* is the effective mass of the charge carriers, which usually decreases with increasing carrier mobility, and n is the charge carrier concentration.

From **Equation 3**, it is clear that the Seebeck coefficient is mainly affected by the carrier concentration and carrier mobility. The well-known trade-off relationship between the Seebeck coefficient and electrical conductivity of thermoelectric materials is not observed in this study. With a moderate amount of dopant, the carrier mobility is enhanced through the carrier filtering effect and this allows the Seebeck coefficient to increase without suppressing electrical conductivity. [15] Figure 1f shows that 23 wt% is an optimal lignin dopant concentration, and that the highest Seebeck coefficient is 98.9 μVK^{-1}, with a power factor of 132.2 $\mu Wm^{-1}K^{-2}$. For comparison purposes, we tabulate power factors of similar multi-walled carbon nanotube (MWCNT)-based thermoelectric composites from recent studies, in **Table 1**. Comparing with other studies based on MWCNTs, the values of CNTY/lignin nanocomposites reported here are at least two orders of magnitude higher than the state of the art, indicating that lignin is an extremely effective doping agent for MWCNTs. The only exception is MWCNT-PDDA/MWCNT-DOC/PEDOT, which exhibits slightly higher PF than that of CNTY/lignin in the present study, due to the high content of PEDOT, and the combination of LbL assembly with electrochemical polymerization to create synergy capable of producing a high power factor. [16]

2.3. Thermoelectric Generator

To prove the concept, a TEG device was assembled using CNTY/lignin nanocomposites, as shown in **Figure 2**a. The power output was evaluated using a

constant temperature gradient of 20 °C and 30 °C, as shown in Figure 2b. The TEG consists of 20 legs on a copper substrate and exhibited a moderate output current of 0.4 mA at a temperature gradient of 20 °C, resulting in an output power of 2.2 μW. Increasing the temperature gradient to 30 °C leads to a corresponding increase in output current and a maximum power of 3.8 μW is reached. The maximum power is given for a circuit resistance of 11 Ω which indicates a real applicability in current electronic devices since their internal resistance is in that range. This represent one of the highest values reported to date taking into account the number on thermoelectric elements and the temperature gradient applied. This TEG can be used in a medium range temperature gradient applications until 180^{o}C as maximum operational temperature. At temperatures higher than 180^{o}C, lignin crosslinking and degradation process occur which can be translated in a detriment of power generated by the thermoelectric device.

3. Conclusion

Lignin was used as a dopant to prepare CNTY-based nanocomposites via simply mixing. The prepared nanocomposites were characterised in terms of structure and thermoelectric performance while the effect of dopant concentration was studied. With a moderate dopant concentration, lignin molecules can densify CNTY bundles through strong π–π interactions forming an interconnected nanostructure. The equilibrium energy band at the CNTY/lignin interface reduces the energy barrier, therefore inducing a carrier filtering effect, and this leads to enhanced charge transport within CNTY/lignin nanocomposites. With a 23 wt% lignin dopant concentration, both the electrical conductivity and Seebeck coefficient were doubled when compared to pristine CNTYs, reaching values of 135.1 S/cm and 98.9 μV/K respectively. This results in a remarkable power factor of 132.2 μW/K^{2}m, more than six fold of the pristine

CNTYs. A TEG device comprising twenty 1-mm-long CNTY/lignin nanocomposite yarns was fabricated, and a maximum power output of 3.8 μW at a temperature gradient of 30 K was recorded. These results suggest that high performance thermoelectric nanocomposite materials can be easily synthesised using a readily available waste stream as dopant. Overall, these findings represent an opportunity for underutilised lignin valorisation showing its potential as an advanced material for next generation thermoelectric devices which can be both cost effective and sustainable. This work definitely contribute to the current challenge of lignin valorisation through high end value products. This new class of lignin nanocomposites will open the gate for future investigations in the field of thermoelectric generators, exploring new pathways to maximize the thermoelectric efficiency of carbon based semiconductors using different type of lignins and how its different molecular structure affects their semiconducting behaviour. This will allow the possibility to have a myriad of biobased nanocomposites to manufacture thermometric devices even with both types of semiconductors (n y p type)

4. Experimental Section

Materials: CNTYs are synthesised by the direct spinning method, whereby an aerogel of CNTs are drawn out of a reactor as a filament via chemical vapour deposition. [17] Synthesis conditions were adjusted to produce few-layer MWCNTs with average outer diameter of 5nm, as reported previously. [18] Multiple individual CNT filaments were overlapped, creating unidirectional yarn-like strings. [19] The lignin used in this study is Alcell extracted using the Organosolv process and was supplied as solid powder (Tecnaro, Germany). The molecular weight (M_w) was measured to be 4000 g/mol and the glass transition temperature (Tg) was recorded at 100 °C.

Preparation of CNTY/lignin nanocomposites: Impregnation was utilised to dope the CNTYs with lignin. Lignin was first dissolved in tetrahydrofuran (THF) at the following concentrations: 1.25 wt%, 2.5 wt%, 5 wt%, 10 wt% and 20 wt% and then 2-mm-long CNTYs were suspended in solutions for 5 minutes before drying in an oven at 70^{o}C for 1 hour. Specimens were weighed before and after impregnation to determine the lignin concentration in newly fabricated nanocomposites, as shown in **Table 2**.

Characterisation: The Seebeck coefficient was determined utilising a custom built in-house system as demonstrated in **Figure 3**a. Temperature gradients were generated via two Peltier modules controlled with a BSI PSM 3/2A DC power supply. The temperature difference (ΔT) between two ends of the specimen was recorded using thermocouples, whilst the voltage (ΔV) generated due to the Seebeck effect was measured by a FLUKE 8842A multimetre. The Seebeck coefficient (S) was calculated using the following equation:

$$S = \frac{\Delta V}{\Delta T} \quad (4)$$

Electrical conductivity was measured using the four point probe method, as shown in Figure 3b, and in accordance to the following equation:

$$\sigma = \frac{ln2}{\pi w R} \quad (5)$$

where w is the yarn diameter, and R is the resistance of the yarn. [20]

The power factor (PF) of CNTY/lignin nanocomposites was calculated using **Equation 2**.

The structural and cross-sectional morphology of the CNTYs were characterized utilising a Hitachi SU-70 scanning electron microscope using the field emission mode (FE-SEM) at 5.00 - 10.00 kV.

A TEG consisting of 20 legs with each leg measuring 1cm length were connected in two parallel series and assembled using CNTY/lignin bio-nanocomposite yarns, as shown in **Figure 6**. For each series, yarns were electrically connected via copper wires with silver paint was applied to ensure good contact. The TEG was assembled at room humidity and temperature conditions and was then mounted on a copper plate, which is rendered thermally insulate by coating with silicon glue. The total dimensions of TEG were 2x5x1 cm. The copper plate was then heated on a heating plate to generate a temperature gradient between the upper end and lower end of the CNTYs. A FLIR One infrared camera was used to determine the temperature at each end. The voltage and current generated by the TEG device were measured between two terminated copper wires using a FLUKE 8842A multimetre with a range of circuit resistance from 1 Ω to 100 Ω, controlled by adjusting the resistors connected to the circuit. The resistance of the TEG device was also measured.

The power output (P) was determined using the following equation:

$$P = \frac{V^2}{R} = I^2 R \qquad (6)$$

where V is the measured voltage, I is the measured current, and R is the measured resistance of the TEG device. The power measurements were carried out at room temperature and humidity conductions. Two different temperature gradients were apply (20 and 30 K) using a hot plate to generate the voltage associated to the thermoelectric effect of the TEG.

References

[1] D. M. Rowe, *Thermoelectrics handbook: macro to nano*, CRC press, **2018**.

[2] a) M. Culebras, C. M. Gómez, A. Cantarero, *J. Mater. Chem. A* **2014**, 2, 10109; b) M. Culebras, C. Gómez, A. Cantarero, *Materials* **2014**, 7, 6701; c) M. Culebras, B. Uriol, C. M. Gomez, A. Cantarero, *Phys. Chem. Chem. Phys.* **2015**, 17, 15140; d) M. Culebras, M. M. de Lima, C. Gómez, A. Cantarero, *Journal of Applied Polymer Science* **2016**, DOI: 10.1002/app.43927n/a; e) J. Gao, C. Liu, L. Miao, X. Wang, C. Li, R. Huang, Y. Chen, S. Tanemura, *Synth. Met.* **2015**, 210, 342; f) H. Shi, C. Liu, J. Xu, H. Song, B. Lu, F. Jiang, W. Zhou, G. Zhang, Q. Jiang, *ACS Appl Mater Interfaces* **2013**, 5, 12811; g) M. Culebras, A. M. Igual-Muñoz, C. Rodríguez-Fernández, M. I. Gómez-Gómez, C. Gomez, A. Cantarero, *ACS applied materials & interfaces* **2017**, 9, 20826.

[3] a) J. P. Heremans, V. Jovovic, E. S. Toberer, A. Saramat, K. Kurosaki, A. Charoenphakdee, S. Yamanaka, G. J. Snyder, *Science* **2008**, 321, 554; b) O. Caballero-Calero, P. Díaz-Chao, B. Abad, C. V. Manzano, M. D. Ynsa, J. J. Romero, M. M. Rojo, M. S. Martín-González, *Electrochim. Acta* **2014**, 123, 117.

[4] G. Carotenuto, C. L. Hison, F. Capezzuto, M. Palomba, P. Perlo, P. Conte, *J. Nanopart. Res.* **2008**, 11, 1729.

[5] T. C. Harman, P. J. Taylor, M. P. Walsh, B. E. LaForge, *Science* **2002**, 297, 2229.

[6] X. W. Wang, H. Lee, Y. C. Lan, G. H. Zhu, G. Joshi, D. Z. Wang, J. Yang, A. J. Muto, M. Y. Tang, J. Klatsky, S. Song, M. S. Dresselhaus, G. Chen, Z. F. Ren, *Appl. Phys. Lett.* **2008**, 93, 193121.

[7] M. Culebras, K. Choi, C. Cho, *Micromachines* **2018**, 9, 638.

[8] J. L. Blackburn, A. J. Ferguson, C. Cho, J. C. Grunlan, *Advanced Materials* **2018**, 30.

[9] a) K. Koziol, J. Vilatela, A. Moisala, M. Motta, P. Cunniff, M. Sennett, A. Windle, *Science* **2007**, 318, 1892; b) N. Behabtu, C. C. Young, D. E. Tsentalovich, O. Kleinerman, X. Wang, A. W. K. Ma, E. A. Bengio, R. F. ter Waarbeek, J. J. de Jong, R. E. Hoogerwerf, S. B. Fairchild, J. B. Ferguson, B. Maruyama, J. Kono, Y. Talmon, Y. Cohen, M. J. Otto, M. Pasquali, *Science* **2013**, 339, 182.

[10] a) E. Senokos, V. Reguero, J. Palma, J. J. Vilatela, R. Marcilla, *Nanoscale* **2016**, 8, 3620; b) J. C. Fernández‐Toribio, A. Íñiguez‐Rábago, J. Vilà, C. González, Á. Ridruejo, J. J. Vilatela, *Advanced Functional Materials* **2016**, 26, 7139; c) Y. Zhao, J. Q. Wei, R. Vajtai, P. M. Ajayan, E. V. Barrera, *Sci Rep-Uk* **2011**, 1.

[11] H. Mainka, O. Täger, E. Körner, L. Hilfert, S. Busse, F. T. Edelmann, A. S. Herrmann, *Journal of Materials Research and Technology* **2015**, 4, 283.

[12] a) S. Kubo, J. F. Kadla, *Macromolecules* **2004**, 37, 6904; b) J. F. Kadla, S. Kubo, *Composites Part A: Applied Science and Manufacturing* **2004**, 35, 395; c) S. Kubo, J. Kadla, *Journal of Polymers and the Environment* **2005**, 13, 97; d) Suhas, P. J. M. Carrott, M. M. L. Ribeiro Carrott, *Bioresource Technology* **2007**, 98, 2301; e) C. Wang, S. S. Kelley, R. A. Venditti, *ChemSusChem* **2016**, 9, 770; f) W. Fang, S. Yang, X.-L. Wang, T.-Q. Yuan, R.-C. Sun, *Green Chemistry* **2017**, 19, 1794; g) S. Gillet, M. Aguedo, L. Petitjean, A. R. C. Morais, A. M. da Costa Lopes, R. M. Łukasik, P. T. Anastas, *Green Chemistry* **2017**, 19, 4200.

[13] Y. H. Kang, U. H. Lee, I. H. Jung, S. C. Yoon, S. Y. Cho, *Acs Appl Electron Ma* **2019**, 1, 1282.

[14] a) G. H. Kim, L. Shao, K. Zhang, K. P. Pipe, *Nat Mater* **2013**, 12, 719; b) G. Kim, K. P. Pipe, *Phys Rev B* **2012**, 86.

[15] C. Cho, M. Culebras, K. L. Wallace, Y. X. Song, K. Holder, J. H. Hsu, C. Yu, J. C. Grunlan, *Nano Energy* **2016**, 28, 426.

[16] M. Culebras, C. Cho, M. Krecker, R. Smith, Y. X. Song, C. M. Gomez, A. Cantarero, J. C. Grunlan, *Acs Appl Mater Inter* **2017**, 9, 6306.

[17] Y. L. Li, I. A. Kinloch, A. H. Windle, *Science* **2004**, 304, 276.

[18] V. Reguero, B. Aleman, B. Mas, J. J. Vilatela, *Chem Mater* **2014**, 26, 3550.

[19] D. Iglesias, E. Senokos, B. Aleman, L. Cabana, C. Navio, R. Marcilla, M. Prato, J. J. Vilatela, S. Marchesan, *Acs Appl Mater Inter* **2018**, 10, 5760.

[20] A. Ramadan, R. Gould, A. Ashour, *Thin Solid Films* **1994**, 239, 272.

[21] C. Z. Meng, C. H. Liu, S. S. Fan, *Adv Mater* **2010**, 22, 535.

[22] Q. L. Zhang, W. J. Wang, J. L. Li, J. J. Zhu, L. J. Wang, M. F. Zhu, W. Jiang, *J Mater Chem A* **2013**, 1, 12109.

[23] Y. Du, S. Z. Shen, W. D. Yang, K. F. Cai, P. S. Casey, *Synthetic Met* **2012**, 162, 375.

[24] L. Tzounis, T. Gartner, M. Liebscher, P. Potschke, M. Stamm, B. Voit, G. Heinrich, *Polymer* **2014**, 55, 5381.

[25] H. J. Song, K. F. Cai, J. Wang, S. Shen, *Synthetic Met* **2016**, 211, 58.

[26] M. Aghelinejad, S. N. Leung, *Compos Part B-Eng* **2018**, 145, 100.

[27] P. Slobodian, P. Riha, R. Olejnik, M. Kovar, P. Svoboda, *J Nanomater* **2013**, DOI: Artn 792875

10.1155/2013/792875.

[28] R. Sarabia-Riquelme, J. Craddock, E. A. Morris, D. Eaton, R. Andrews, J. Anthony, M. C. Weisenberger, *Synthetic Met* **2017**, 225, 86.

[29] C. Bounioux, P. Diaz-Chao, M. Campoy-Quiles, M. S. Martin-Gonzalez, A. R. Goni, R. Yerushalmi-Rozene, C. Muller, *Energ Environ Sci* **2013**, 6, 918.

[30] Q. Wu, J. L. Hu, *Compos Part B-Eng* **2016**, 107, 59.

[31] Z. Zhang, G. M. Chen, H. F. Wang, X. Li, *Chem-Asian J* **2015**, 10, 149.

[32] Y. C. Sun, D. Terakita, A. C. Tseng, H. E. Naguib, *Smart Mater Struct* **2015**, 24.

Figure 1. FE-SEM images of surface morphology of (a) pristine CNTY and (b) CNTY/lignin nanocomposite doped with 34 wt% lignin; schematic diagrams of (c) densified WMCNT fibre microstructure by incorporating lignin, (e) charge carrier filtering mechanism by introducing lignin; thermoelectric properties of CNTY/lignin nanocomposites with varying dopant levels: (d) electrical conductivity, (f) Seebeck coefficient and power factor.

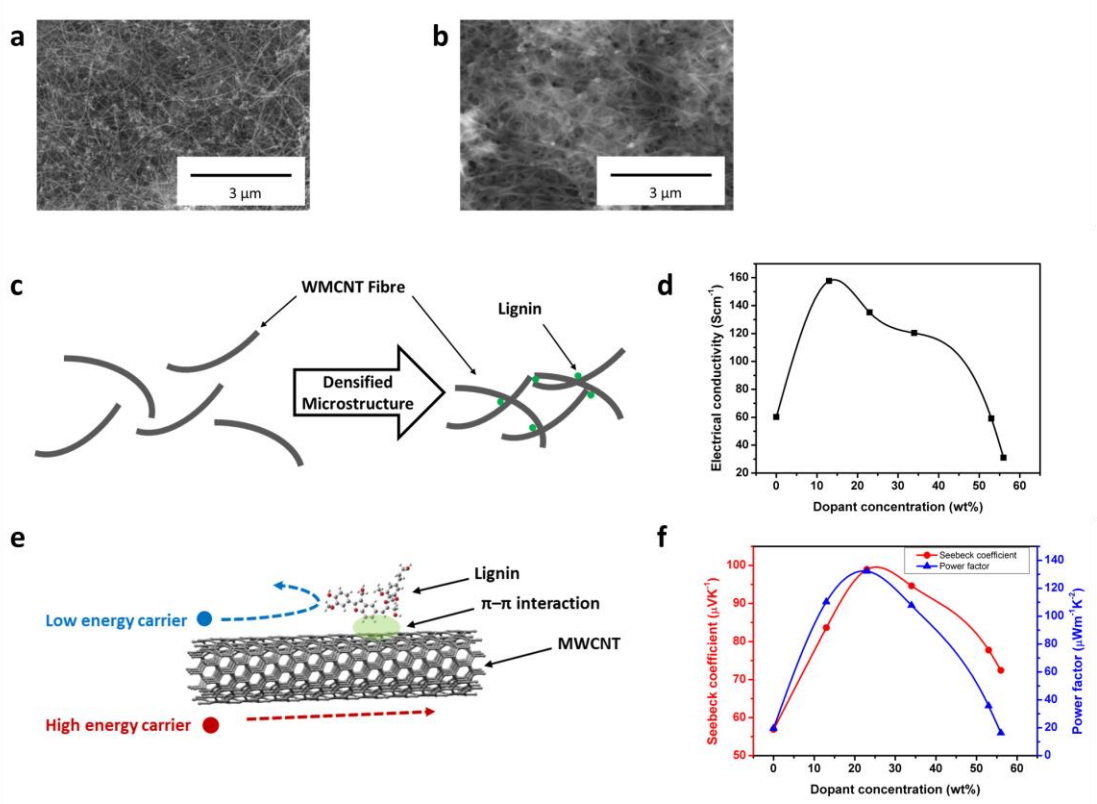

Figure 2. (a) Schematic of the assembled TEG device using CNTY/lignin nanocomposite and (b) its output power curves at temperature gradients of 20 °C and 30 °C.

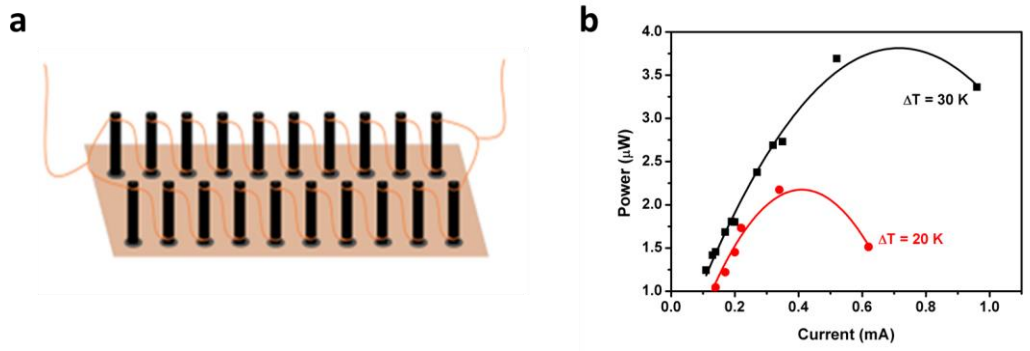

Figure 3. Schematic of the experimental set-up for (a) Seebeck coefficient measurement and (b) resistance measurement

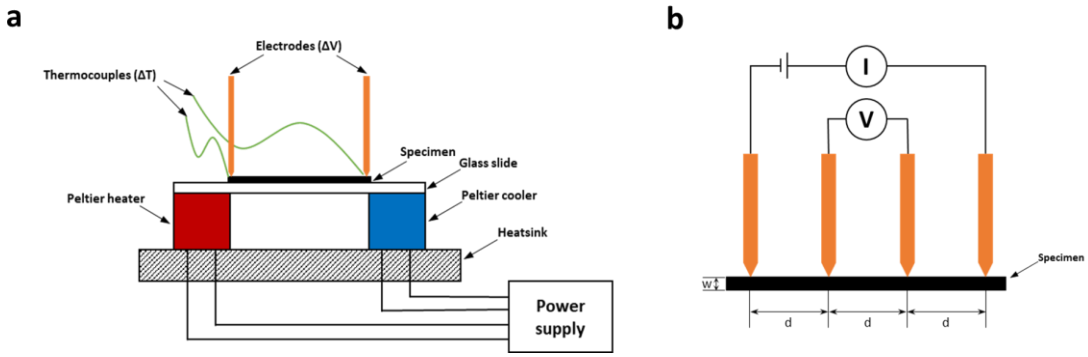

Table 1. Summary of the power factors of MWCNT-based thermoelectric composites.

Materials	Preparation method	PF ($\mu Wm^{-1}K^{-2}$)	Ref.
CNTY/lignin	Mixing	132.2	This study
PANI/MWCNT	In-situ polymerization	5	[21]
PANI/MWCNT	Mixing	1.07×10^{-1}	[22]
MWCNT/P3HT	In-situ polymerization	1.56×10^{-3}	[23]
PC/MWCNT-COOH/CBT	In-situ polymerization	7.60×10^{-6}	[24]
MWCNT/PPy	In-situ polymerization	2.2	[25]
PVDF/MWCNT	In-situ polymerization	2.03×10^{-3}	[26]
PVDF/PPy/MWCNT	In-situ polymerization	2.16×10^{-3}	[26]
MWCNT/EOC	Mixing	2.30×10^{-5}	[27]
MWCNT/ PVP	Mixing	0.6	[28]
PEI/MWCNT/ PVP	Mixing	1.98	[28]
P3HT/MWCNT	Mixing	6	[29]
WPU/MWCNT/PEDOT:PSS	Mixing	1.41	[30]
PEDOT:PSS/MWCNT	In-situ polymerization	2.29×10^{-1}	[31]
MWCNT/Nafion	Mixing	0.75	[32]
MWCNT-PDDA/MWCNT-DOC/PEDOT	LbL + In-situ polymerization	155	[16]

Table 2. Lignin concentration in solution and nanocomposite

Lignin concentration in solution (wt%)	Lignin concentration in nanocomposite (wt%)
1.25	13
2.5	23
5	34
10	53
20	56